

6-30-2023

## Effects of Hydrogen/Deuterium Exchange on Protein Stability in Solution and in the Gas Phase

Yousef Haidar  
yhaidar2@uwo.ca

Lars Konermann  
konermann, konerman@uwo.ca

Follow this and additional works at: <https://ir.lib.uwo.ca/chempub>

 Part of the [Chemistry Commons](#)

---

### Citation of this paper:

Haidar, Yousef and Konermann, Lars, "Effects of Hydrogen/Deuterium Exchange on Protein Stability in Solution and in the Gas Phase" (2023). *Chemistry Publications*. 270.  
<https://ir.lib.uwo.ca/chempub/270>

# **Effects of Hydrogen/Deuterium Exchange on Protein**

## **Stability in Solution and in the Gas Phase**

Yousef Haidar and Lars Konermann\*

*Department of Chemistry, The University of Western Ontario, London, Ontario,*

*N6A 5B7, Canada*

\* corresponding author: [konerman@uwo.ca](mailto:konerman@uwo.ca)

**Abstract.** Mass spectrometry (MS)-based techniques are widely used for probing protein structure and dynamics in solution. H/D exchange (HDX)-MS is one of the most common approaches in this context. HDX is often considered to be a “benign” labeling method, in that it does not perturb protein behavior in solution. However, several studies have reported that D<sub>2</sub>O pushes unfolding equilibria toward the native state. The origin, and even the existence of this protein stabilization remain controversial. Here we conducted thermal unfolding assays in solution to confirm that deuterated proteins in D<sub>2</sub>O are more stable, with 2 – 4 K higher melting temperatures than unlabeled proteins in H<sub>2</sub>O. Previous studies tentatively attributed this phenomenon to strengthened H-bonds after deuteration, an effect that may arise from the lower zero-point vibrational energy of the deuterated species. Specifically, it was proposed that strengthened water-water bonds (W··W) in D<sub>2</sub>O lower the solubility of nonpolar side chains. The current work takes a broader view by noting that protein stability in solution also depends on water-protein (W··P) and protein-protein (P··P) H-bonds. To help unravel these contributions, we performed collision-induced unfolding (CIU) experiments on gaseous proteins generated by native electrospray ionization. CIU profiles of deuterated and unlabeled proteins were indistinguishable, implying that P··P contacts are insensitive to deuteration. Thus, protein stabilization in D<sub>2</sub>O is attributable to solvent effects, rather than alterations of intraprotein H-bonds. Strengthening of W··W contacts represents one possible explanation, but the stabilizing effect of D<sub>2</sub>O can also originate from weakened W··P bonds. Future work will be required to elucidate which of these two scenarios is correct, or if both contribute to protein stabilization in D<sub>2</sub>O. In any case, the often-repeated adage that “D-bonds are more stable than H-bonds” does not apply to intramolecular contacts in native proteins.

## Introduction

Native proteins in solution are stabilized by numerous noncovalent contacts. Two key factors are backbone H-bonds that mediate the formation of secondary structure, and the hydrophobic effect which causes the clustering of nonpolar residues in the protein core.<sup>1-3</sup> Salt bridges and other contacts play a role as well. Together, these interactions counteract the destabilizing effects of conformational entropy, such that the native state N is favored over the unfolded state U under physiological conditions ( $\Delta G_U > 0$  for  $N \rightleftharpoons U$ ).

Condensed phase techniques that provide atomically-resolved protein structures include X-ray crystallography, nuclear magnetic resonance (NMR) spectroscopy, and cryo-electron microscopy.<sup>4</sup> Complementary insights come from mass spectrometry (MS)-based techniques, such as covalent labeling<sup>5-7</sup> and crosslinking.<sup>8,9</sup> A concern with the latter two strategies is the possibility that covalent modifications can perturb the protein behavior, such that labeling or crosslinking patterns might not fully reflect the properties of the native state.<sup>10</sup> This potential problem necessitates careful controls to ensure the absence of artifacts.<sup>8,11</sup>

H/D exchange (HDX) experiments with MS or NMR detection represent another important tool for probing protein structure and dynamics.<sup>12,13</sup> In these studies, the protein is incubated in D<sub>2</sub>O-based labeling buffer, triggering the exchange of N, O, and S-linked protium (H) with deuterium (D). HDX in exposed side chains proceeds on a sub-second time scale. H-bonded backbone sites exchange more slowly, requiring seconds to weeks at physiological pH.<sup>14</sup> This slow backbone deuteration is mediated by dynamic protein motions.<sup>12,13</sup>

Compared to covalent labeling or crosslinking, HDX is less intrusive. Many HDX studies implicitly assume that replacing H with D is completely benign and does not affect protein structure and dynamics.<sup>15</sup> However, this is not necessarily true. Compared to H<sub>2</sub>O, D<sub>2</sub>O has a 10% higher viscosity, 10% higher maximum density, and 7 K higher temperature of maximum density.<sup>16</sup> These

differences can affect the properties of H-bonded systems.<sup>17</sup> A number of studies have reported that protein incubation in D<sub>2</sub>O stabilizes the native state, evident from an increased melting temperature ( $T_m$ )<sup>18-21</sup> and a larger (more positive)  $\Delta G_U$ .<sup>18-20</sup> D<sub>2</sub>O can also suppress protein dynamic motions.<sup>22,23</sup>

The origin<sup>18,19,24</sup> and extent<sup>25</sup> of protein stabilization in D<sub>2</sub>O remain controversial. Several studies have attributed D<sub>2</sub>O-induced stabilization to enhancement of the hydrophobic effect in D<sub>2</sub>O, i.e., a lower solubility of nonpolar side chains in D<sub>2</sub>O compared to H<sub>2</sub>O.<sup>20,26</sup> This scenario may arise from stronger “H”-bonds among solvent molecules, i.e., stronger DOD $\cdots$ OD<sub>2</sub> contacts compared to HOH $\cdots$ OH<sub>2</sub>.<sup>26-29</sup> Indeed, gaseous D<sub>2</sub>O dimers are more stable than H<sub>2</sub>O dimers, an effect that is related to shifts in the zero-point vibrational energy (ZPVE).<sup>30-32</sup>

Understanding ZPVE effects on H-bond stability is not straightforward. A harmonic oscillator has  $ZPVE = \frac{1}{2}h\nu$  with the frequency  $\nu = (2\pi)^{-1} (K/m)^{1/2}$ , where  $h$  is Planck’s constant and  $K$  is the force constant.<sup>33</sup> Replacing a vibrating H-atom with D lowers ZPVE, because  $m_D > m_H$ . However, a lower ZPVE does not necessarily strengthen H-bonds. The enthalpy  $\Delta H_{HB}$  of H-bond dissociation  $XH\cdots Y \rightarrow XH + Y$  may increase, decrease, or stay the same upon deuteration. The direction and magnitude of the stability change depends on whether the bound or the unbound state experiences a larger ZPVE shift (Figure 1). The situation becomes even more complicated in large systems with many vibrational modes, particularly in the presence of charges.<sup>34</sup> In such cases, the stability trend can be reversed, making D-bonds more stable than H-bonds.<sup>35</sup> It has also been noted that D- vs. H-bond stability differences are most prevalent at cryogenic temperatures, while entropic factors diminish this difference under ambient conditions.<sup>36</sup> In addition, the dissociation of one bond often allows the formation of another bond, e.g., when backbone NH $\cdots$ OC contacts are replaced with water-protein bonds upon unfolding.<sup>37</sup> Overall, the mechanism of protein stabilization in D<sub>2</sub>O remains elusive, although the purported higher stability of D-bonds vs. H-bonds features prominently in most explanation attempts.<sup>18-20,24,26-28</sup>

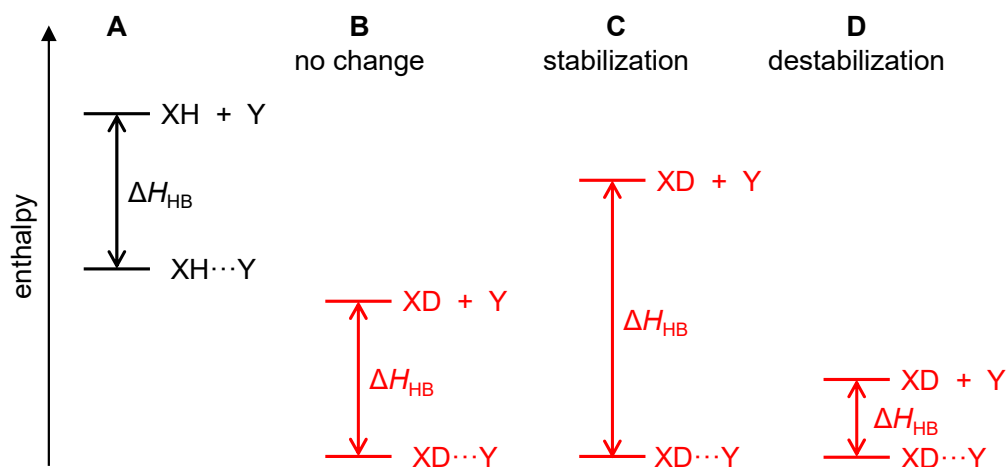


**Figure 1.** Schematic illustration of possible deuteration-induced effects on the H-bond strength  $\Delta H_{\text{HB}}$ . Horizontal lines represent zero-point vibrational energies (ZPVEs) of the bound and dissociated states. (A)  $\Delta H_{\text{HB}}$  prior to deuteration. (B) Deuteration lowers both ZPVEs equally;  $\Delta H_{\text{HB}}$  remains unchanged. (C) ZPVE of the bound state gets lowered more than that of the dissociated state;  $\Delta H_{\text{HB}}$  increases. (D) ZPVE of the dissociated state gets lowered more than that of the bound state;  $\Delta H_{\text{HB}}$  decreases.

We propose that it should be possible to streamline the discussion of protein stabilization in D<sub>2</sub>O by dissecting H-bonds into three categories:<sup>38,39</sup> (i) Water-water (W··W) bonds, i.e., DOD··OD<sub>2</sub> vs. HOH··OH<sub>2</sub>. (ii) Water-protein (W··P) bonds, i.e., D<sub>2</sub>O··protein vs. H<sub>2</sub>O··protein. (iii) Intramolecular protein-protein (P··P) bonds. Category (iii) comprises both backbone (ND··OC vs. NH··OC) as well as side chain H-bonds. Backbone P··P bonds are a key contributor to protein folding and stability,<sup>40</sup> although side chain P··P contacts can contribute as well.<sup>41,42</sup> The secondary role of the latter reflects the fact that most charged/polar side chains protrude into the solvent, rendering the formation of P··P bonds sterically difficult.<sup>43-45</sup>

With only a few exceptions,<sup>38,46</sup> previous discussions focused on W··W bonds<sup>18-20,24,26-28</sup> while ignoring the possible involvement of other factors. In particular, it has not been possible to uncover the relevance of P··P bonds, partly because many samples had either incomplete<sup>20</sup> or poorly controlled backbone deuteration.<sup>29,38,47,48</sup>

The premise of the current work is that it should be possible to separate the role of P··P bonds from the solvent-linked contributions (W··W and W··P) by examining solvent-free proteins. Under native ESI conditions (non-denaturing solutions, minimal collisional excitation), solution-like protein structures survive in the gas phase,<sup>49-53</sup> with retention of most backbone H-bonds, on the millisecond time scale of typical ion mobility spectrometry (IMS) measurements.<sup>54-57</sup> The stability of gaseous proteins generated by native ESI can be assessed in collision-induced unfolding (CIU) experiments, where conformational changes are detected by IMS.<sup>58-65</sup> Thus, comparative CIU experiments on deuterated and unlabeled protein ions should reveal whether the stability of P··P bonds is subject to isotope effects. The observation of deuteration-induced stabilization in the gas phase would suggest that P··P bonds also cause stabilization of deuterated proteins in D<sub>2</sub>O solution. Conversely, the absence of deuteration-induced stabilization in the gas phase would imply that solvent contributions (W··W and/or W··P) are responsible for the higher stability of proteins in D<sub>2</sub>O.

By conducting thermal unfolding experiments on fully deuterated proteins in D<sub>2</sub>O and H<sub>2</sub>O solution, the current work confirms the existence of D<sub>2</sub>O-induced stabilization. However, deuterated and unlabeled gaseous protein ions exhibited indistinguishable stability. We conclude that protein stabilization in D<sub>2</sub>O is caused solely by solvent effects.

## **Materials and Methods**

**Materials and Sample Preparation.** Equine heart cytochrome *c* (cyt *c*, 12360 Da), hen egg white lysozyme (14305 Da), and bovine ubiquitin (8565 Da) were supplied by Millipore Sigma (St. Louis, MO). D<sub>2</sub>O was from Isowater (Collingwood, ON). All other chemicals were purchased from Thermo Fisher Scientific (Mississauga, ON). An AB15 glass electrode pH-meter (Fisher) was used for pH measurements; pD values referenced throughout this work are glass electrode readings that were

corrected according to  $pD = (pH \text{ meter reading}) + 0.4$ .<sup>66</sup> Protein stock solutions (500  $\mu\text{M}$ ) were initially dialyzed for 24 h against water for removal of salt contaminants using 10 kDa MWCO Millipore Sigma dialysis cassettes. Deuteration was performed by incubating protein samples in 99%  $\text{D}_2\text{O}$  at 42  $^\circ\text{C}$  for three weeks, at a protein concentration of 5  $\mu\text{M}$  (10  $\mu\text{M}$  for *cyt c*) and pD 5.3 in 10 mM  $\text{D}_2\text{O}$ -based acetate buffer. Sodium acetate was used in optical experiments to ensure consistency with earlier unfolding experiments,<sup>67</sup> whereas ammonium acetate was used for ESI-MS. Unlabeled samples were treated exactly the same way, except that  $\text{H}_2\text{O}$  was used for all steps instead of  $\text{D}_2\text{O}$ . Control experiments revealed that  $\text{D}_2\text{O}$  incubation periods beyond three weeks did not further enhance the deuteration percentage.

**Unfolding in Solution.** Thermal unfolding experiments were performed with circular dichroism (CD) spectroscopy detection on a Jasco J-810 instrument (Easton, MD) with a 1 mm cuvette using 5  $\mu\text{M}$  lysozyme and 10  $\mu\text{M}$  *cyt c*. The ellipticity was measured at 222 nm (which reports on  $\alpha$ -helicity<sup>68</sup>), while heating the solutions from 21  $^\circ\text{C}$  to 100  $^\circ\text{C}$  at 1  $^\circ\text{C min}^{-1}$ . The ellipticity at 222 nm is commonly used for thermal unfolding experiments because it yields a relatively high S/N ratio.<sup>69</sup> In comparison, the 250-300 nm range (which reports on tertiary structure) produces signals that are  $\sim 2$  orders of magnitude less intense.<sup>70</sup> Also, the proteins studied here have been shown to undergo two-state thermal unfolding,<sup>25,67,71</sup> such that different CD wavelengths will provide the same information.<sup>37,69</sup> Unfolding experiments in  $\text{H}_2\text{O}$  were performed at pH 4.9 and pH 5.3, and in  $\text{D}_2\text{O}$  at pD 5.3. All measurements were conducted in triplicate. Experimentally measured ellipticities  $\theta$  for all temperatures  $T$  were converted to normalized ellipticity  $\theta_{\text{norm}}$  according to

$$\theta_{\text{norm}} = \frac{\theta - \theta_N}{\theta_U - \theta_N} \quad (1)$$



where  $\theta_N$  and the  $\theta_U$  are the ellipticities of the native and unfolded protein at 21° C and 100° C, respectively. Thermodynamic parameters were determined by fitting the  $\theta_{\text{norm}}$  profiles using<sup>37,69</sup>

$$\theta_{\text{norm}} = \frac{(y_N + m_N T) + (y_U + m_U T) \exp\left(-\frac{\Delta G_U}{RT}\right)}{1 + \exp\left(-\frac{\Delta G_U}{RT}\right)} \quad (2)$$

where

$$\Delta G_U = \Delta H_U \left(1 - \frac{T}{T_m}\right) \quad (3)$$

is the free energy of the  $N \rightleftharpoons U$  unfolding equilibrium, and  $\Delta H_U$  is the corresponding enthalpy. The  $(y_N + m_N T)$  and  $(y_U + m_U T)$  terms in eq. 2 represent the pre- and post-transition baselines. Least square fitting was performed using custom-designed Microsoft Excel worksheets, employing the Solver routine for nonlinear generalized reduced gradient minimization. From the fitted  $\Delta H_U$  and  $T_m$  parameters, one can calculate the fraction of unfolded protein in solution  $f_{U\_SOL}$  as

$$f_{U\_SOL} = \frac{[U]}{[N] + [U]} = \frac{\exp\left(-\frac{\Delta G_U}{RT}\right)}{1 + \exp\left(-\frac{\Delta G_U}{RT}\right)} \quad (4)$$

Keeping in mind that  $0 = \Delta H_U - T_m \Delta S_U$ , the entropy of unfolding ( $\Delta S_U$ ) is

$$\Delta S_U = \frac{\Delta H_U}{T_m} \quad (5)$$

Eqs. 1-5 are widely used for analyzing thermal protein unfolding in solution,<sup>37,69</sup> but the fitted parameters  $\Delta G_U$ ,  $\Delta H_U$ , and  $\Delta S_U$  are only valid in the vicinity of  $T_m$  because this strategy does not consider the temperature dependence of enthalpy and entropy.

**Native Mass Spectrometry and Ion Mobility Spectrometry.** ESI-IMS/MS experiments were performed on a SYNAPT G2 instrument in positive ion mode (Waters, Milford, MA) with the ESI capillary held at 2.8 kV. Proteins in H<sub>2</sub>O or D<sub>2</sub>O solution were infused at room temperature using a syringe pump at 5  $\mu\text{L min}^{-1}$ . Temperatures and voltages were adjusted to ensure minimum thermal and collision excitation during ion sampling (source 30 °C, desolvation gas 40 °C, sampling cone 5 V, extraction cone 3 V). For a full list of instrument settings, see Table S1.

CIU was performed after quadrupole selection of the most intense charge states for each protein. Collisional excitation was implemented by varying the trap collision voltage  $V_{\text{trap}}$  between 2 V and 70 V with Ar as a collision gas. To ensure that unlabeled and deuterated protein ions experienced collisions with equivalent center-of-mass translational energies  $E_{\text{COM}}$ , we used the relationship  $E_{\text{COM}} = E_{\text{LAB}} m_{\text{Ar}} / (m_{\text{Prot}} + m_{\text{Ar}}) \approx E_{\text{LAB}} m_{\text{Ar}} / m_{\text{Prot}}$  where  $m_{\text{Ar}}$  is the mass of Ar,  $m_{\text{Prot}}$  is the mass of the protein, and  $E_{\text{LAB}} = z \times e \times V_{\text{trap}}$  is the laboratory-frame translational energy.<sup>72,73</sup> Accordingly,  $V_{\text{trap}}$  was increased for deuterated samples by a factor of  $m_{\text{Prot}}(\text{deuterated}) / m_{\text{Prot}}(\text{unlabeled})$ . For example, excitation of unlabeled ubiquitin (8565 Da) with  $V_{\text{trap}} = 50$  V is equivalent to excitation of deuterated ubiquitin with  $V_{\text{trap}} = 50 \text{ V} \times (8565 + 142) / 8565 = 50.8$  V. For simplicity,  $V_{\text{trap}}$  settings will be reported as nominal values, i.e., for the example used here, both the corrected and the uncorrected value would be given as “50 V”.

Protein conformational changes triggered by collisional excitation were probed by travelling wave IMS (TWIMS) with N<sub>2</sub> as the primary buffer gas. TWIMS drift times were converted to effective He collision cross sections ( $^{\text{TW}}\text{CCS}_{\text{N}_2 \rightarrow \text{He}}$ , referred to as “ $\Omega$ ” throughout this work).<sup>74,75</sup> Average collision cross sections  $\langle \Omega \rangle$  were calculated from the measured  $\Omega$  distributions. The extent of CIU was quantified by calculating the fraction of unfolding in vacuum,  $f_{\text{U\_VAC}}$ , according to

$$f_{\text{U\_VAC}} = \frac{\langle \Omega \rangle - \langle \Omega \rangle_{\text{N}}}{\langle \Omega \rangle_{\text{U}} - \langle \Omega \rangle_{\text{N}}} \quad (6)$$

where  $\langle\Omega\rangle_N$  represents the average collision cross section of the folded protein ions at  $V_{\text{trap}} = 2$  V, while  $\langle\Omega\rangle_U$  represents the average collision cross section of the unfolded ions at  $V_{\text{trap}} = 70$  V. All CIU experiments were performed in triplicate with independent  $\Omega$  calibrations. Error bars represent standard deviations.

## Results and Discussion

Protein thermal stability assays in neutral solution tend to be challenging because unfolding often takes place close to the boiling point of water. A common strategy for mitigating this problem is to lower  $T_m$  by mild acidification.<sup>67,71</sup> The current work focused on *cyt c*, lysozyme, and ubiquitin. These three are representative of many other globular proteins,<sup>43-45</sup> and they have been widely studied in earlier gas phase<sup>54,55,57,58,61,63,76-79</sup> and solution investigations.<sup>15,67,71,80</sup> Our experiments were conducted at pH (and pD) 5.3, which is well within the stability range of all three proteins at room temperature.<sup>15,80</sup> Preliminary tests (not shown) revealed that thermal unfolding in solution was straightforward for *cyt c* and lysozyme at pH 5.3. However, ubiquitin is very resilient even at low pH,<sup>43,67</sup> such that we were unable to characterize thermal unfolding of this protein in solution. The high stability of ubiquitin has been attributed to its tight H-bonding network and compact hydrophobic core.<sup>43</sup> The subsequent sections will therefore discuss solution data only for *cyt c* and lysozyme, while ESI-MS and IMS/MS results are shown for all three proteins.

**Native ESI Mass Spectra in H<sub>2</sub>O and D<sub>2</sub>O.** ESI mass spectra of *cyt c*, lysozyme, and ubiquitin acquired in H<sub>2</sub>O at pH 5.3 are depicted in Figure 2 (black traces). All three spectra show  $[M + zH]^{z+}$

ions in low charge states that are consistent with tightly folded solution conformations, as seen in earlier native ESI experiments.<sup>55,76,77,81,82</sup>

Protein deuteration was performed as outlined in the Methods section, and the resulting samples were electrosprayed in D<sub>2</sub>O solution. The charge state distributions of the deuterated [M + zD]<sup>z+</sup> ions (Figure 2, red traces) were virtually identical to those of the [M + zH]<sup>z+</sup> ions electrosprayed in H<sub>2</sub>O. This high degree of similarity indicates that the release of protein ions into the gas phase and the associated charging mechanism(s) are insensitive to isotope effects. The extent of deuteration was measured from the most intense peaks in the spectra (insets of Figure 2). Deuteration percentages were determined using  $\%D = (\Delta M_{\text{exp}} / \Delta M_{\text{max}})$ , where  $\Delta M_{\text{exp}}$  is the experimentally measured mass shift.  $\Delta M_{\text{max}}$  is the maximum possible mass shift for complete deuteration of all exchangeable sites (backbone, side chains, termini, and the two heme propionates in cyt *c*; the cyt *c* N-terminus is acetylated<sup>45</sup>).  $\Delta M_{\text{max}}$  values for cyt *c*, lysozyme, and ubiquitin are 195, 255, and 144 Da, respectively. The average %D value obtained in this way was (96 ± 2.5)%. Considering that proteins can undergo some gas phase back exchange during ESI and ion sampling,<sup>83,84</sup> we conclude that the D<sub>2</sub>O labeling strategy used here generates proteins that are essentially fully deuterated. This is in contrast to several earlier studies on proteins in H<sub>2</sub>O vs. D<sub>2</sub>O, where deuteration was incomplete, poorly controlled, or unreported.<sup>20,29,47,48</sup>

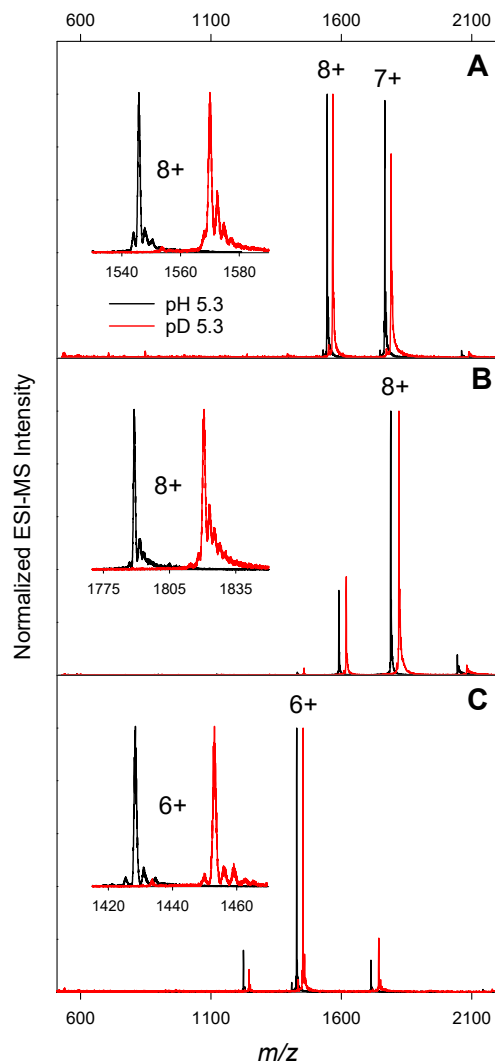


**Figure 2.** Native mass spectra of (A) cyt *c*, (B) lysozyme, (C) ubiquitin electrosprayed in H<sub>2</sub>O solution (black, pH 5.3), and fully deuterated samples in D<sub>2</sub>O solution (red, pD 5.3). All samples contained 10 mM ammonium acetate. Selected peaks are labeled with their charge state.

**pH Effects on Thermal Protein Unfolding.** Prior to conducting comparative stability measurements in H<sub>2</sub>O vs. D<sub>2</sub>O, it is necessary to examine a potential source of artifacts. Like most earlier investigations, we used the relationship  $pD = (pH\text{-meter reading}) + 0.4$  to prepare solutions with equivalent H<sup>+</sup> and D<sup>+</sup> activity.<sup>15,20-22,66</sup> Thus, we compared samples at pH 5.3 and pD 5.3 (the latter having a pH-meter reading of 4.9). However, the appropriateness of this “+ 0.4 correction” has been questioned, prompting some studies to rely on uncorrected pH-meter readings in D<sub>2</sub>O.<sup>19,25,85</sup> In other words, there is

a possibility that protein stability comparisons in H<sub>2</sub>O vs. D<sub>2</sub>O might be skewed by differences in H<sup>+</sup> and D<sup>+</sup> activity. To explore the severity of this issue we examined the worst-case scenario, where the effective acidity differs by 0.4 units. To this end, we initially performed stability measurements in H<sub>2</sub>O solution at pH 5.3 and pH 4.9.

CD-detected thermal unfolding curves of *cyt c* and lysozyme at pH 5.3 and pH 4.9 are depicted in Figure 3A, D. Visual inspection of the experimental and fitted  $\theta_{\text{norm}}$  data reveals subtle differences for both proteins upon changing pH by 0.4 units (black and blue in Figure 3A, D). However, closer analysis reveals that the  $T_m$  values of both proteins remain unchanged, within experimental error. Both proteins exhibit a slightly higher  $\Delta H_U$  at pH 5.3, but even this alteration remains close to the measurement uncertainty (Table 1). The  $f_U$  profiles (Figure 3B, E) as well as the corresponding  $\Delta G_U(T)$  data (Figure 3 C, F) are nearly superimposable at pH 4.9 and pH 5.3. We conclude that the thermal unfolding behavior of *cyt c* and lysozyme is virtually identical when conducting the experiments at pH 4.9 and pH 5.3. In other words, the disputed validity<sup>19,25</sup> of the “+ 0.4 correction” is not an issue under the conditions of this work. We therefore continued to rely on this correction throughout this work, consistent with most other studies in the field.<sup>15,20-22,66</sup>

**D<sub>2</sub>O-Mediated Protein Stabilization in Solution.** While numerous studies have reported that D<sub>2</sub>O enhances the thermodynamic stability of native proteins in solution,<sup>18-22,26</sup> there are also voices that have questioned the existence of this effect (see e.g. Figure 1C in ref. <sup>25</sup>, which suggests that D<sub>2</sub>O causes protein destabilization). Instead of relying on these partially conflicting literature data, we sought to verify the occurrence of stability difference in H<sub>2</sub>O vs. D<sub>2</sub>O ourselves.

CD-detected unfolding profiles of fully deuterated *cyt c* and lysozyme acquired at pD 5.3 showed a notable shift to higher temperatures, compared to profiles measured at pH 5.3 (black vs. red data in Figure 3A, D). The D<sub>2</sub>O-induced  $T_m$  increase for the two proteins was 2.0 K and 4.2 K,

respectively. Thermodynamic stabilization of both proteins is evident from an upward displacement of the  $\Delta G_U$  profiles in D<sub>2</sub>O relative to H<sub>2</sub>O (Figure 3C, F), implying that the N  $\rightleftharpoons$  U equilibria were shifted toward the native state in D<sub>2</sub>O. This D<sub>2</sub>O-induced stabilization is consistent with earlier results.<sup>18-22,26</sup> Overall, the results of Figure 3 confirm that *cyt c* and lysozyme are more thermodynamically stable in D<sub>2</sub>O than in H<sub>2</sub>O. In contrast to some earlier studies, this result was obtained for samples that had well controlled (virtually complete) deuteration, as seen from the mass shifts in Figure 2. We also verified that the observed isotope effect is independent of possible differences in the H<sup>+</sup> vs. D<sup>+</sup> activity, as discussed in the preceding section.

The free energy of unfolding is  $\Delta G_U = \Delta H_U - T\Delta S_U$ , allowing us to determine the enthalpic and entropic contributions to D<sub>2</sub>O-induced stabilization. Table 1 reveals that D<sub>2</sub>O-exposure causes  $\Delta H_U$  to increase by 40 kJ mol<sup>-1</sup> and 60 kJ mol<sup>-1</sup> for *cyt c* and lysozyme, respectively. This enthalpic stabilization of the native state in D<sub>2</sub>O is in line with earlier reports.<sup>18-20</sup> Interestingly, enthalpic stabilization is counteracted by a  $\Delta S_U$  increase in D<sub>2</sub>O of ca. 100 J K<sup>-1</sup> mol<sup>-1</sup> which destabilizes the native state. The occurrence of this enthalpy-entropy compensation in H<sub>2</sub>O vs. D<sub>2</sub>O has been noted earlier.<sup>25</sup> However, the fact that  $\Delta G_U$  is more positive in D<sub>2</sub>O than in H<sub>2</sub>O (Figure 3C, F) implies that the stabilizing  $\Delta\Delta H_U > 0$  dominates over the destabilizing  $\Delta\Delta S_U > 0$ .

In the absence of additional information, it is difficult to interpret D<sub>2</sub>O-induced  $\Delta H_U$  and  $\Delta S_U$  effects of Table 1 because proteins in solution experience numerous intra- and intermolecular contacts, all of which have enthalpic and entropic contributions.<sup>19,37</sup> In particular, it is not possible to unravel whether the D<sub>2</sub>O-induced net stabilization is related to solvent effects (W $\cdots$ W and W $\cdots$ P bonds, see Introduction), or by the strengthening of H-bonds within the proteins (P $\cdots$ P bonds). The gas phase experiments discussed in the following section help unravel this puzzle.

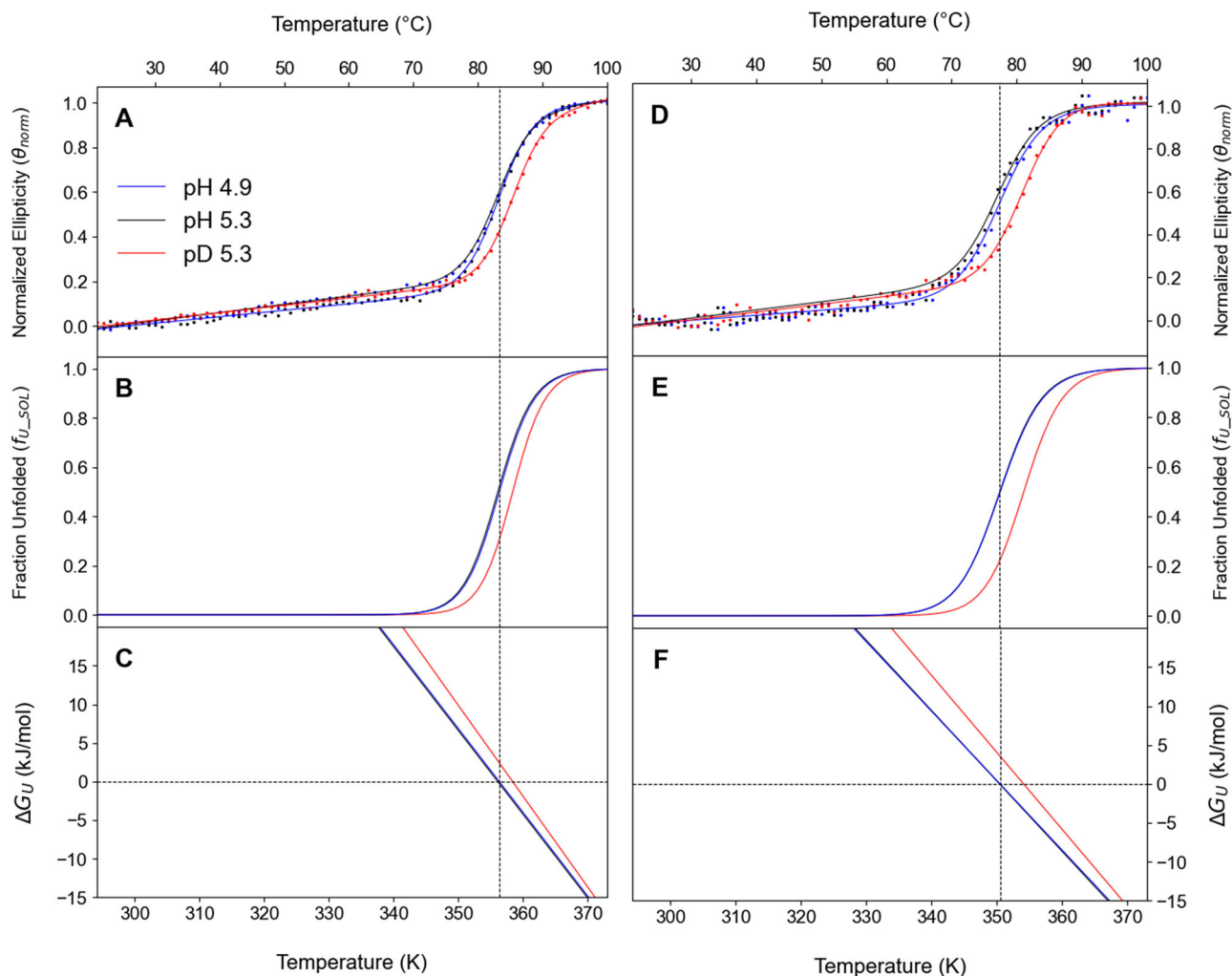


**Figure 3.** Thermodynamic analyses of cyt *c* (A-C) and lysozyme (D-F) thermal unfolding in H<sub>2</sub>O and in D<sub>2</sub>O solution. Colors denote pH 4.9 (blue), pH 5.3 (black), and pD 5.3 (red). Panels A, D show experimental CD unfolding profiles (dots) and the corresponding eq. 2 fits. Panels B, E depict the fraction of unfolded protein  $f_{U\_SOL}$  vs. temperature (eq. 4), while panels C, F show free energy profiles. Vertical dashed lines indicate  $T_m$  values in H<sub>2</sub>O.



**Table 1.** Thermodynamic parameters determined from thermal unfolding experiments (Figure 3) on cyt *c* and lysozyme in H<sub>2</sub>O and D<sub>2</sub>O solution.

	cyt <i>c</i>			lysozyme		
	$T_m$ (K)	$\Delta H_U$ (kJ mol <sup>-1</sup> )	$\Delta S_U$ (J K <sup>-1</sup> mol <sup>-1</sup> )	$T_m$ (K)	$\Delta H_U$ (kJ mol <sup>-1</sup> )	$\Delta S_U$ (J K <sup>-1</sup> mol <sup>-1</sup> )
pH 4.9	356.4 ± 0.5	380 ± 10	1070 ± 40	350.9 ± 0.5	290 ± 10	814 ± 40
pH 5.3	356.4 ± 0.7	390 ± 20	1080 ± 70	350.2 ± 0.7	310 ± 10	920 ± 40
pD 5.3	358.4 ± 0.5	430 ± 10	1190 ± 40	354.4 ± 0.3	370 ± 20	1040 ± 30

**Unfolding of Unlabeled and Deuterated Proteins in the Gas Phase.** We examined the CIU behavior of the most intense protein ions generated by native ESI, i.e., cyt *c* 8+, lysozyme 8+, and ubiquitin 6+. IMS profiles were acquired for  $V_{\text{trap}}$  values between 2 V and 70 V. Gas phase collisional excitation triggered large-scale unfolding, evident from shifts of the IMS distribution to higher  $\Omega$  (Figure 4). For  $V_{\text{trap}}$  beyond 65 V the spectral quality started to deteriorate as a result of collision-induced dissociation (CID), i.e., covalent bond rupture events that are commonly observed when performing CIU with high collision energy.<sup>86,87</sup>

CIU of cyt *c* and ubiquitin proceeded via semi-unfolded intermediate structures, evident from features in-between the most compact and the fully unfolded species (e.g., Figures 4C, K). In contrast, lysozyme CIU took place without distinct intermediates. The relative increase in  $\langle\Omega\rangle$  during CIU was smaller for lysozyme (21%) than for cyt *c* (49%) and ubiquitin (38%). This behavior reflects the presence of four disulfide bridges that limit the conformational freedom of unfolded lysozyme.<sup>44</sup> Neither cyt *c* nor ubiquitin possess disulfide bridges,<sup>43,45</sup> allowing these two proteins to adopt more expanded conformations after CIU. Overall, the gas phase unfolding behavior seen in Figure 4 for all three proteins agrees with previous native IMS/MS data acquired with H<sub>2</sub>O solutions.<sup>61,64,78</sup>

A key result of our CIU experiments is that unlabeled and deuterated protein ions exhibited IMS data that were virtually indistinguishable from one another throughout the entire range of  $V_{\text{trap}}$  values, evident from the overlapping black and red profiles in Figure 4. Numerous additional  $V_{\text{trap}}$  values were tested, and these data were compiled into  $f_{\text{U\_VAC}}$  profiles that reflect the extent of gas phase unfolding (Figure 5). These  $f_{\text{U\_VAC}}$  data reaffirm that the CIU behavior of all three protein ions is independent of their deuteration status. The insensitivity of gas phase protein unfolding to isotope effects (Figures 4, 5) is in striking contrast to the behavior in solution, where D<sub>2</sub>O significantly stabilizes the native state (Figure 3).<sup>18-21</sup> It appears that this is the first time that the CIU behavior of unlabeled vs. deuterated proteins has been compared directly.

**Implications of H-Bonds vs. D-Bonds for Protein Stability in the Gas Phase.** The compact gas phase conformers populated in native ESI experiments with minimum collision excitation ( $V_{\text{trap}} = 2$  V in Figure 4) retain much of their solution secondary and tertiary structure, along with preservation of most backbone NH $\cdots$ OC hydrogen bonds.<sup>49-52,54-57</sup> Additionally, these gas phase proteins form new intramolecular H-bonds as part of salt bridges on the protein surface, resulting from the collapse of formerly extended titratable side chains.<sup>54,56,79,88</sup> CIU of these compact protein ions generates significantly expanded conformers at the CID threshold that have lost much of their secondary and tertiary structure, and where most backbone and side chain H-bonds (D-bonds) have been disrupted or rearranged.<sup>89,90</sup> Our CIU data reveal that there is no stability difference for unlabeled vs. deuterated proteins, implying that the dissociation energy of P $\cdots$ P bonds in gaseous protein ions is not affected by the bridging atom (H vs. D). This finding does not support the view that D-bonds are generally more stable than H-bonds.<sup>30-32</sup> Instead, our data suggest that P $\cdots$ P bonds behave in accordance with the scenario of Figure 1B. This finding applies to both, backbone P $\cdots$ P bonds that already existed in solution, as well as side chain P $\cdots$ P bonds formed after protein desolvation during

ESI.<sup>54,56,79,88</sup> D-induced stabilization has previously been found to be prevalent in small, neutral systems, such as H<sub>2</sub>O dimers.<sup>35</sup> Thus, the absence of deuteration-induced stabilization in electrosprayed protein ions (i.e., large systems with a net charge) is not completely unexpected.

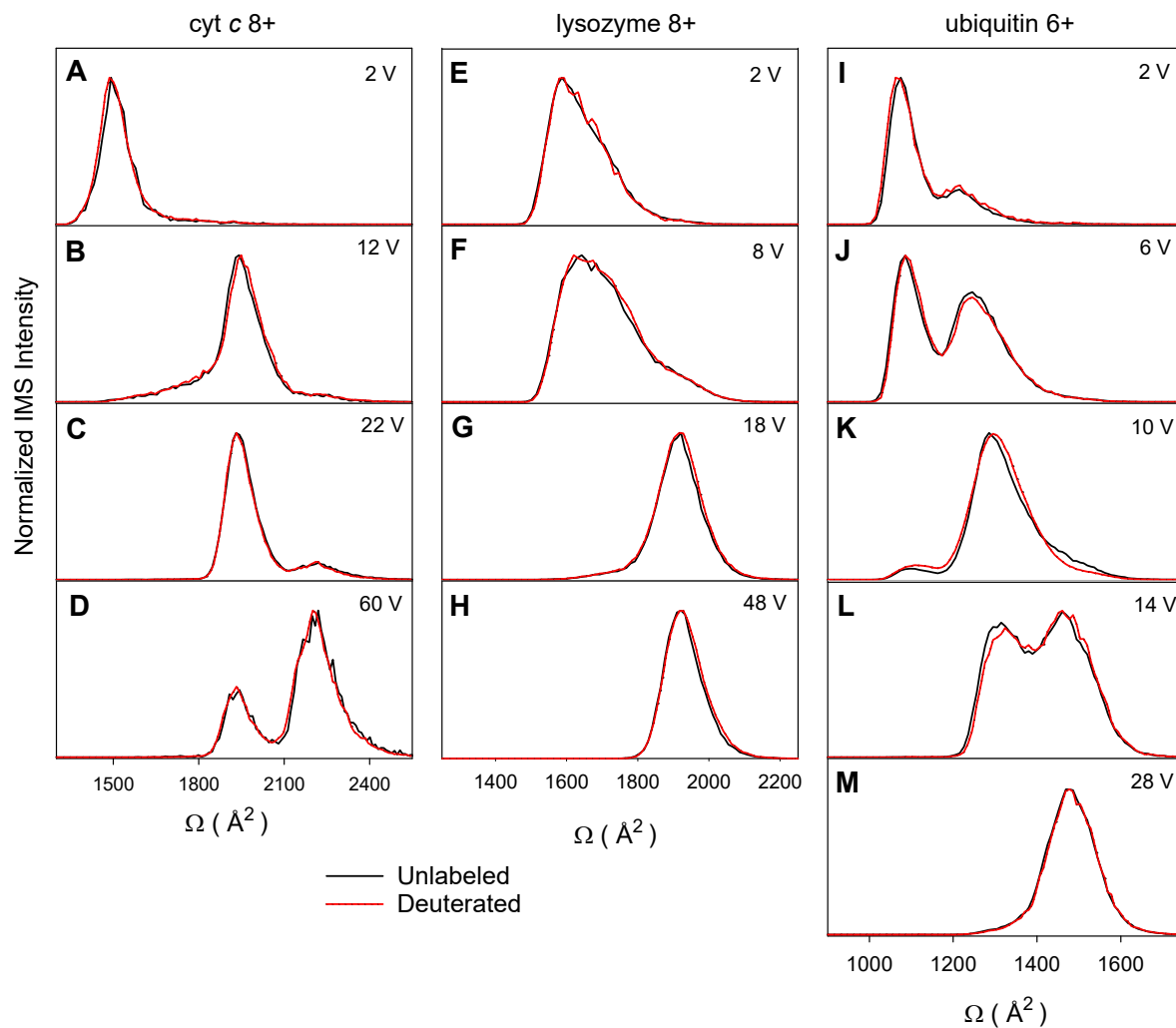


**Figure 4.** CIU data, displaying collision cross section ( $\Omega$ ) distributions for unlabeled (black) and deuterated (red) gaseous protein ions at different levels of collisional heating. The trap collision voltage  $V_{\text{trap}}$  is indicated in each panel. (A-D) cyt c 8+, (E-H) lysozyme 8+, and (I-M) ubiquitin 6+.

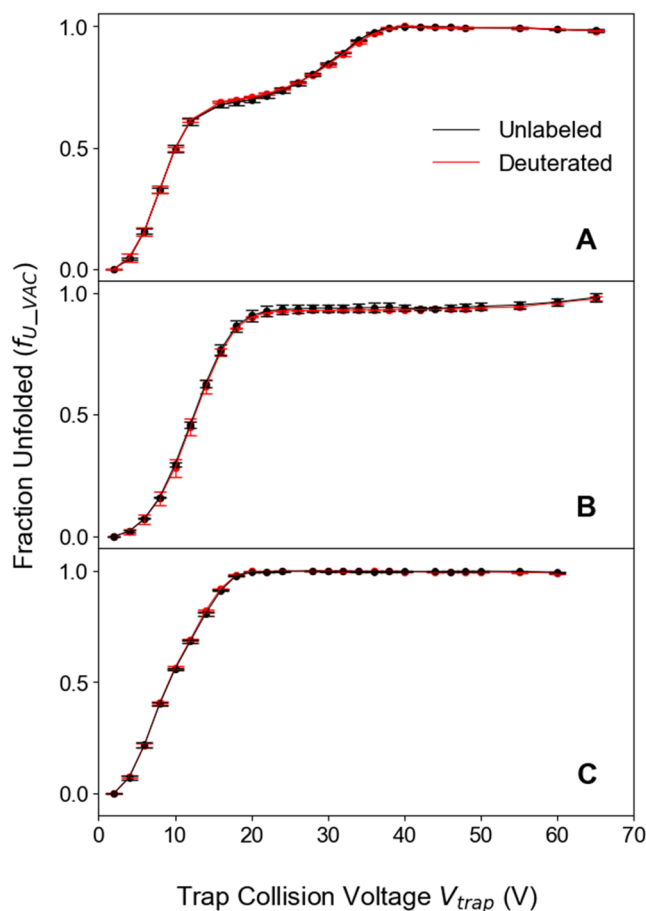


**Figure 5.** CIU profiles of deuterated vs. unlabeled (A) *cyt c* 8+, (B) lysozyme 8+, and (C) ubiquitin 6+ ions generated by native ESI. The profiles were calculated from  $\Omega$  values acquired at different  $V_{\text{trap}}$ , with subsequent normalization via eq. 6.

**Dissecting Isotope Effects on Protein Stability.** Toy models can illustrate basic protein concepts.<sup>91,92</sup> Here, we use a two-dimensional lattice chain model for examining a  $N \rightleftharpoons U$  equilibrium in solution (Figure 6). Within the model, water molecules (blue) can form up to four H-bonds, hydrophilic residues (red) can form two H-bonds, while hydrophobic residues (green) can form only one H-bond. We assume that for any protein structure, the system will form the maximum possible number of H-bonds, i.e.,  $W \cdots W$ ,  $W \cdots P$ , and  $P \cdots P$  contacts. The number of H-bonds in each category is  $n_{WW}$ ,  $n_{WP}$ , and  $n_{PP}$ , respectively. The corresponding H-bond dissociation enthalpies are

$\Delta H_{\text{HB}}^{\text{WW}}$ ,  $\Delta H_{\text{HB}}^{\text{WP}}$ , and  $\Delta H_{\text{HB}}^{\text{PP}}$ , all of which are positive (Figure 1). A more detailed discussion might consider the possibility that not all  $\Delta H_{\text{HB}}$  values within each group are identical. However, for the simple analysis conducted here, the use of just three  $\Delta H_{\text{HB}}$  values will suffice.

Just like for actual proteins,<sup>43-45</sup> the native state in our model has a hydrophobic core and a hydrophilic exterior (Figure 6A). The total number of H-bonds in this structure is 110. Unfolding exposes hydrophobic residues to water, thereby lowering the total number of H-bonds to 108. Thus, the model correctly captures the fact that unfolding in solution leads to a net loss of H-bonds, a factor that contributes to the hydrophobic effect.<sup>37</sup> Because D<sub>2</sub>O-induced protein stabilization is caused by enthalpy (Table 1),<sup>18-20</sup> our discussion only focuses on  $\Delta H_{\text{U}}$  effects, while not examining  $\Delta S_{\text{U}}$ -related factors.  $\Delta H_{\text{U}}$  in our model is given by

$$\Delta H_{\text{U}} = -\Delta n_{\text{WW}} \Delta H_{\text{HB}}^{\text{WW}} - \Delta n_{\text{WP}} \Delta H_{\text{HB}}^{\text{WP}} - \Delta n_{\text{PP}} \Delta H_{\text{HB}}^{\text{PP}} \quad (7)$$

Comparison of Figures 6A and 6B reveals that  $n_{\text{PP}}$  decreases to zero as the protein unfolds. These broken intramolecular contacts are then replaced with newly formed W·P bonds, causing  $n_{\text{WP}}$  to increase. Intrusion the unfolded chain into the water network lowers the number of W·W bonds, i.e.  $n_{\text{WW}}$  decreases. These trends also apply to actual proteins,<sup>37</sup> although the magnitude of the  $\Delta n$  terms is system-dependent. For our model,  $\Delta n_{\text{WW}} = -9$ ,  $\Delta n_{\text{WP}} = 14$ , and  $\Delta n_{\text{PP}} = -7$ , such that

$$\Delta H_{\text{U}} = 9 \Delta H_{\text{HB}}^{\text{WW}} - 14 \Delta H_{\text{HB}}^{\text{WP}} + 7 \Delta H_{\text{HB}}^{\text{PP}} \quad (8)$$

The data in Table 1 demonstrate that protein stabilization in D<sub>2</sub>O results from a shift of  $\Delta H_{\text{U}}$  to more positive values ( $\Delta \Delta H_{\text{U}} > 0$ ). Eq. 8 reveals that this stabilization may be caused by three factors, i.e., an increase of  $\Delta H_{\text{HB}}^{\text{WW}}$ , a decrease of  $\Delta H_{\text{HB}}^{\text{WP}}$ , or an increase of  $\Delta H_{\text{HB}}^{\text{PP}}$ .

Which of these three possibilities is most likely? The CIU data of Figures 4 and 5 show that  $\Delta H_{\text{HB}}^{\text{PP}}$  is insensitive to isotope effects, such that this possibility can be excluded (Figure 1B). Early

work indicated that D<sub>2</sub>O enhances the hydrophobic effect by lowering the solubility of nonpolar side chains, suggesting that  $\Delta H_{\text{HB}}^{\text{WW}}$  increases in D<sub>2</sub>O (Figure 1C).<sup>26</sup> However, subsequent studies found the opposite trend, i.e., higher or identical solubilities of nonpolar molecules in D<sub>2</sub>O vs. H<sub>2</sub>O (ref. <sup>24</sup> and references therein). These later findings cast doubt on the traditional belief that  $\Delta H_{\text{HB}}^{\text{WW}}$  increases in bulk D<sub>2</sub>O, even though this stability trend holds for isolated D<sub>2</sub>O dimers.<sup>30-32</sup>

A possible resolution of this conundrum is that  $\Delta H_{\text{HB}}^{\text{WP}}$  decreases in D<sub>2</sub>O solution, a scenario that has not thus far been considered in the literature. While our data do not provide conclusive proof for weakened W··P contacts as the cause of protein stabilization in D<sub>2</sub>O, it appears that this scenario is consistent with all of the available data. As noted in Figure 1D, such a destabilization of H-bonds is well within the realm of possible outcomes after HDX.<sup>34,35</sup>

## Conclusions

60+ years after its discovery,<sup>26</sup> the stabilization of proteins in D<sub>2</sub>O remains poorly understood. In agreement with earlier work, we found that this stabilization is rooted in enthalpic effects, i.e., a larger (more positive) value of  $\Delta H_U$  in D<sub>2</sub>O than in H<sub>2</sub>O.<sup>18-20</sup> Like those earlier studies, we attribute this stabilization to changes in the dissociation enthalpy of H-bonds. This effect is countered by entropy, as  $\Delta S_U$  is larger (more positive) in D<sub>2</sub>O than in H<sub>2</sub>O, thereby causing destabilization (Table 1). However, the  $\Delta H_U$  term dominates, resulting in a net stabilization of the native state in D<sub>2</sub>O. While previous studies focused almost exclusively on W··W bonds,<sup>18-20,24,26-28</sup> we took a broader approach and also considered the role of W··P and P··P bonds, because stability changes in all three categories can affect the protein behavior in D<sub>2</sub>O (Figure 6).

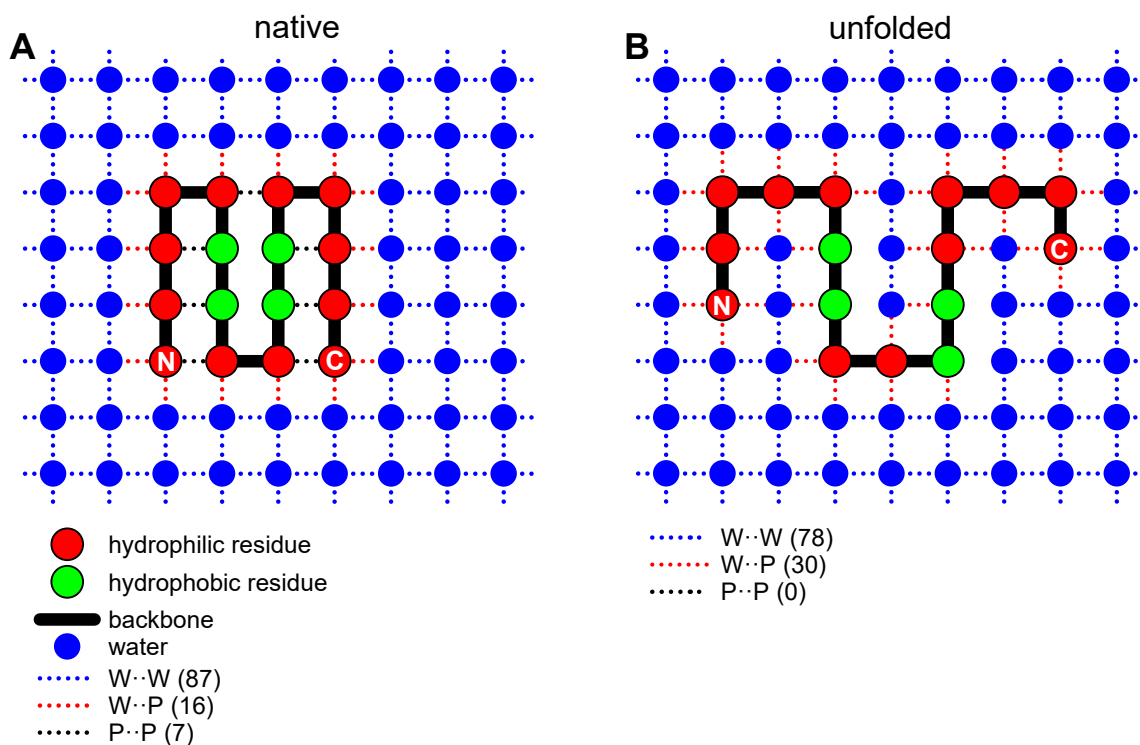


**Figure 6.** Two-dimensional lattice bead chain model of a protein in water. (A) Native protein. (B) Example of an unfolded conformation. Hydrophilic (red) and hydrophobic (green) residues are linked by backbone bonds (solid black line). Termini are marked as “N” and “C”. Blue spheres represent water. H-bonds are indicated as dotted lines of three types (W··W, W··P, P··P). The corresponding  $n_{\text{HB}}$  values are shown in brackets. Bonds around the periphery of the lattice were not included in the  $n_{\text{HB}}$  counts.

As far as we are aware, this work marks the first time that the stability of deuterated and unlabeled proteins has been examined *in vacuo* (although isotope effects on gaseous protein-ligand complexes have been explored earlier).<sup>93</sup> Our CIU experiments revealed that the stability of gaseous proteins is indistinguishable before and after deuteration, demonstrating that P··P bonds are insensitive to isotope effects. It can be concluded that protein stabilization in D<sub>2</sub>O arises either from strengthened W··W bonds, or from weakened W··P bonds (a combination of both scenarios is possible as well). Strengthening of W··W bonds has been favored in the earlier literature.<sup>18-20,26-28</sup> However, weakening of W··P bonds seems just as likely, especially when considering the results of more recent solubility studies (ref. <sup>24</sup> and references therein). Thus, while we cannot conclusively

determine the mechanistic basis of protein stabilization in D<sub>2</sub>O, our results show that this stabilization is caused by the solvent, rather than H-bonds within the protein.

For HDX-MS and HDX-NMR experiments, our results imply that exposure to D<sub>2</sub>O may alter certain aspects of protein structure and dynamics. The stability differences seen in our solution experiments were detected at relatively high temperatures, around  $T_m$ . Typical HDX experiments use ambient temperature,<sup>12,13</sup> but there is great interest in also using HDX/MS for high temperature measurements.<sup>94,95</sup> D<sub>2</sub>O-induced stability enhancements should be taken into account for the interpretation of such high-temperature HDX data. It is likely that D<sub>2</sub>O-induced stabilization makes its presence felt already at room temperature, e.g., as a rigidification of the native state,<sup>22,23</sup> but more work is required to characterize the extent of these changes. Careful comparison of protein HDX and DHX kinetics<sup>96</sup> are a possible way to explore this aspect in the future.

It is not our intent to question the overall viability of HDX-MS or HDX-NMR for interrogating protein structure and dynamics. After all, the D<sub>2</sub>O-mediated stability enhancements seen here are relatively modest. Also, many HDX studies employ a comparative strategy (e.g., by examining a wild type vs. mutant protein in identical solvent environments). For such comparative studies, both conditions will likely be affected by D<sub>2</sub>O to a similar extent, such that differences in protein behavior should be largely independent of isotope effects.

Complementary to HDX in solution, gas phase HDX can probe electrosprayed proteins in a solvent-free environment.<sup>97-100</sup> It is reassuring that our CIU data did not show any difference for deuterated and unlabeled protein ions, implying that gas phase HDX represents a truly “benign” labeling method that does not perturb protein behavior *in vacuo*. This is in contrast to HDX in solution, where deuteration causes stability changes that are readily observable.



## **Acknowledgments**

We thank Lee-Ann Briere for expert technical assistance with the CD measurements of this work, as well as Elnaz Aliyari for assistance with initial CIU experiments. Funding was provided by the Natural Sciences and Engineering Research Council of Canada (RGPIN-2018-04243).

## **Supporting Information**

Table S1: Instrument settings for TWIMS and CIU experiments.

## References

1. Pace, C.N., Fu, H.L., Fryar, K.L., Landua, J., Trevino, S.R., Schell, D., Thurlkill, R.L., Imura, S., Scholtz, J.M., Gajiwala, K., Sevcik, J., Urbanikova, L., Myers, J.K., Takano, K., Hebert, E.J., Shirley, B.A., Grimsley, G.R.: Contribution of hydrogen bonds to protein stability. *Protein Sci.* **23**, 652-661 (2014)
2. Brini, E., Fennell, C.J., Fernandez-Serra, M., Hribar-Lee, B., Luksic, M., Dill, K.A.: How Water's Properties Are Encoded in Its Molecular Structure and Energies. *Chem. Rev.* **117**, 12385-12414 (2017)
3. Tanford, C.: Contribution of hydrophobic interactions to the stability of the globular conformation of proteins. *J. Am. Chem. Soc.* **84**, 4240-4247 (1962)
4. Dobson, C.M.: Biophysical Techniques in Structural Biology. *Annu. Rev. Biochem.* **88**, 25-33 (2019)
5. Ziemianowicz, D.S., MacCallum, J.L., Schriemer, D.C.: Correlation between Labeling Yield and Surface Accessibility in Covalent Labeling Mass Spectrometry. *J. Am. Soc. Mass Spectrom.* **31**, 207-216 (2020)
6. Sharp, J.S., Chea, E.E., Misra, S.K., Orlando, R., Popov, M., Egan, R.W., Holman, D., Weinberger, S.R.: Flash Oxidation (FOX) System: A Novel Laser-Free Fast Photochemical Oxidation Protein Footprinting Platform. *J. Am. Soc. Mass Spectrom.* **32**, 1601-1609 (2021)
7. Liu, X.R., Zhang, M.M., Gross, M.L.: Mass Spectrometry-Based Protein Footprinting for Higher-Order Structure Analysis: Fundamentals and Applications. *Chem. Rev.* **120**, 4355-4454 (2020)
8. Piersimoni, L., Kastritis, P.L., Arlt, C., Sinz, A.: Cross-Linking Mass Spectrometry for Investigating Protein Conformations and Protein - Protein Interactions—A Method for All Seasons. *Chem. Rev.* **122**, 7500-7531 (2022)
9. Leitner, A., Bonvin, A., Borchers, C.H., Chalkley, R.J., Chamot-Rooke, J., Combe, C.W., Cox, J., Dong, M.Q., Fischer, L., Gotze, M., Gozzo, F.C., Heck, A.J.R., Hoopmann, M.R., Huang, L., Ishihama, Y., Jones, A.R., Kalisman, N., Kohlbacher, O., Mechtler, K., Moritz, R.L., Netz, E., Novak, P., Petrotchenko, E., Sali, A., Scheltema, R.A., Schmidt, C., Schriemer, D., Sinz, A., Sobott, F., Stengel, F., Thalassinou, K., Urlaub, H., Viner, R., Vizzaino, J.A., Wilkins, M.R., Rappsilber, J.: Toward Increased Reliability, Transparency, and Accessibility in Cross-linking Mass Spectrometry. *Structure* **28**, 1259-1268 (2020)
10. Mädler, S., Seitz, M., Robinson, J., Zenobi, R.: Does Chemical Cross-Linking with NHS Esters Reflect the Chemical Equilibrium of Protein-Protein Noncovalent Interactions in Solution? *J. Am. Soc. Mass Spectrom.* **21**, 1775-1783 (2010)
11. Mendoza, V.L., Vachet, R.W.: Probing Protein Structure by Amino Acid-specific Covalent Labeling and Mass Spectrometry. *Mass Spectrom. Rev.* **28**, 785-815 (2009)
12. Masson, G.R., Burke, J.E., Ahn, N.G., Anand, G.S., Borchers, C.H., Brier, S., Bou-Assaf, G.M., Engen, J.R., Englander, S.W., Faber, J.H., Garlish, R.A., Griffin, P.R., Gross, M.L., Guttman, M., Hamuro, Y., Heck, A.J.R., Houde, D., Iacob, R.E., Jorgensen, T.J.D., Kaltashov, I.A., Klinman, J.P., Konermann, L., Man, P., Mayne, L., Pascal, B.D., Reichmann, D., Shekel, M., Snijder, J., Strutzenberg, T.S., Underbakke, E.S., Wagner, C., Wales, T.E., Walters, B.T., Weis, D.D., Wilson, D.J., Wintrode, P.L., Zhang, Z., Zheng, J., Schriemer, D.C., Rand, K.D.: Recommendations for performing, interpreting and reporting hydrogen deuterium exchange mass spectrometry (HDX-MS) experiments. *Nat. Methods* **16**, 595-602 (2019)
13. Deng, B., Lento, C., Wilson, D.J.: Hydrogen deuterium exchange mass spectrometry in biopharmaceutical discovery and development - A review. *Anal. Chim. Acta* **940**, 8-20 (2016)

14. Skinner, J.J., Lim, W.K., Bedard, S., Black, B.E., Englander, S.W.: Protein dynamics viewed by hydrogen exchange. *Protein Sci.* **21**, 996-1005 (2012)
15. Goto, Y., Hagihara, Y., Hamada, D., Hoshino, M., Nishii, I.: Acid-Induced Unfolding and Refolding Transitions of Cytochrome c: A Three-State Mechanism in H<sub>2</sub>O and D<sub>2</sub>O. *Biochemistry* **32**, 11878-11885 (1993)
16. Lide, D.R. *CRC Handbook of Chemistry and Physics* 82nd ed.; CRC Press: Boca Raton, London, New York, Washington, 2001.
17. Shi, C., Zhang, X., Yu, C.-H., Yao, Y.-F., Zhang, W.: Geometric isotope effect of deuteration in a hydrogen-bonded host-guest crystal. *Nat. Commun.* **9**, 481 (2018)
18. Pica, A., Graziano, G.: Effect of heavy water on the conformational stability of globular proteins. *Biopolymers* **109**, 6 (2018)
19. Stadmiller, S.S., Pielak, G.J.: Enthalpic stabilization of an SH3 domain by D<sub>2</sub>O. *Protein Sci.* **27**, 1710-1716 (2018)
20. Efimova, Y.M., Haemers, S., Wierczynski, B., Norde, W., van Well, A.A.: Stability of globular proteins in H<sub>2</sub>O and D<sub>2</sub>O. *Biopolymers* **85**, 264-273 (2007)
21. Hattori, A., Crespi, H.L., Katz, J.J.: Effect of Side-Chain Deuteration on Protein Stability. *Biochemistry* **4**, 1213-1225 (1965)
22. Cioni, P., Strambini, G.B.: Effect on Heavy Water on Protein Flexibility. *Biophys. J.* **82**, 3246-3253 (2002)
23. Panda, D., Chakrabarti, G., Hudson, J., Pigg, K., Miller, H.P., Wilson, L., Himes, R.H.: Suppression of Microtubule Dynamic Instability and Treadmilling by Deuterium Oxide. *Biochemistry* **39**, 5075-5081 (2000)
24. Graziano, G.: Relationship between cohesive energy density and hydrophobicity. *J. Chem. Phys.* **121**, 1878-1882 (2004)
25. Makhatadze, G.I., Clore, G.M., Gronenborn, A.M.: Solvent isotope effect and protein stability. *Nat. Struct. Biol.* **2**, 852-855 (1995)
26. Kresheck, G.C., Schneider, H., Scheraga, H.A.: The Effect of D<sub>2</sub>O on the Thermal Stability of Proteins. Thermodynamic Parameters for the Transfer of Model Compounds from H<sub>2</sub>O to D<sub>2</sub>O. *J. Phys. Chem.* **69**, 3132-3144 (1965)
27. Nemethy, G., Scheraga, H.A.: Structure of Water and Hydrophobic Bonding in Proteins. IV. The Thermodynamic Properties of Liquid Deuterium Oxide. *J. Chem. Phys.* **41**, 680-689 (1964)
28. Parker, M.J., Clarke, A.R.: Amide backbone and water-related H/D isotope effects on the dynamics of a protein folding reaction. *Biochemistry* **36**, 5786-5794 (1997)
29. Henderson, R.F., Henderson, T.R., Woodfin, B.M.: Effects of D<sub>2</sub>O on the Association-Dissociation Equilibrium in Subunit Proteins. *J. Biol. Chem.* **245**, 3733-3737 (1970)
30. Engdahl, A., Nelander, B.: On the relative stabilities of H - and D - bonded water dimers. *J. Chem. Phys.* **86**, 1819-1823 (1987)

31. Clark, T., Heske, J., Kuhne, T.D.: Opposing Electronic and Nuclear Quantum Effects on Hydrogen Bonds in H<sub>2</sub>O and D<sub>2</sub>O. *ChemPhysChem* **20**, 2461-2465 (2019)
32. Wilkinson, F.E., Peschke, M., Szulejko, J.E., McMahon, T.B.: Deuterium isotope effects on gas phase ion-molecule hydrogen-bonding interactions: Alcohol-alkoxide and alcohol-chloride adduct ions. *Int. J. Mass Spectrom.* **175**, 225-240 (1998)
33. Atkins, P. *Physical Chemistry* 10th ed.; W. H. Freeman & Co.: New York, 2010.
34. Buckingham, A.D., Fan-Chen, L.: Differences in the Hydrogen and Deuterium Bonds. *Int. Rev. Phys. Chem.* **1**, 253-269 (1981)
35. Scheiner, S., Cuma, M.: Relative Stability of Hydrogen and Deuterium Bonds. *J. Am. Chem. Soc.* **118**, 1511-1521 (1996)
36. Kjaersgaard, A., Vogt, E., Christensen, N.F., Kjaergaard, H.G.: Attenuated Deuterium Stabilization of Hydrogen-Bound Complexes at Room Temperature. *J. Phys. Chem. A* **124**, 1763-1774 (2020)
37. Fersht, A.R. *Structure and Mechanism in Protein Science*; W. H. Freeman & Co.: New York, 1999.
38. Itzhaki, L.S., Evans, P.A.: Solvent isotope effects on the refolding kinetics of hen egg-white lysozyme. *Protein Sci.* **5**, 140-146 (1996)
39. Frauenfelder, H., Chen, G., Berendzen, J., Fenimore, P.W., Jansson, H., McMahon, B.H., Stroe, I.R., Swenson, J., Young, R.D.: A unified model of protein dynamics. *Proc. Natl. Acad. Sci. U.S.A.* **106**, 5129-5134 (2009)
40. Rose, G.D., Fleming, P.J., Banavar, J.R., Maritan, A.: A backbone-based theory of protein folding. *Proc. Natl. Acad. Sci. U.S.A.* **45**, 16623-16633 (2006)
41. Pace, C.N.: Energetics of protein hydrogen bonds. *Nat. Struct. Mol. Biol.* **16**, 681-682 (2009)
42. Eswar, N., Ramakrishnan, C.: Deterministic features of side-chain main-chain hydrogen bonds in globular protein structures. *Protein Eng.* **13**, 227-238 (2000)
43. Vijay-Kumar, S., Bugg, C.E., Cook, W.J.: Structure of Ubiquitin Refined at 1.8 Å Resolution. *J. Mol. Biol.* **194**, 531-544 (1987)
44. Cheetham, J.C., Artymiuk, P.J., Phillips, D.C.: Refinement of an enzyme complex with inhibitor bound at partial occupancy: Hen egg-white lysozyme and tri-N-acetylchitotriose at 1.75 Å resolution. *J. Mol. Biol.* **224**, 613-628 (1992)
45. Bushnell, G.W., Louie, G.V., Brayer, G.D.: High-resolution Three-dimensional Structure of Horse Heart Cytochrome c. *J. Mol. Biol.* **214**, 585-595 (1990)
46. Guzzi, R., Arcangeli, C., Bizzarri, A.R.: A molecular dynamics simulation study of the solvent isotope effect on copper plastocyanin. *Biophys. Chem.* **82**, 9-22 (1999)
47. Scheraga, H.A.: Helix-Random Coil Transformations in Deuterated Macromolecules. *Ann. NY Acad. Sci.* **84**, 608-616 (1960)
48. Huyghues-Despointes, B.M.P., Scholtz, J.M., Pace, C.N.: Protein conformation stabilities can be determined from hydrogen exchange rates. *Nat. Struct. Biol.* **6**, 910-912 (1999)

49. Tamara, S., den Boer, M.A., Heck, A.J.R.: High-Resolution Native Mass Spectrometry. *Chem. Rev.* **122**, 7269-7326 (2022)
50. Mehmood, S., Allison, T.M., Robinson, C.V.: Mass Spectrometry of Protein Complexes: From Origins to Applications. *Annu. Rev. Phys. Chem.* **66**, 453-474 (2015)
51. Christofi, E., Barran, P.: Ion Mobility Mass Spectrometry (IM-MS) for Structural Biology: Insights Gained by Measuring Mass, Charge, and Collision Cross Section. *Chem. Rev.* **123**, 2902–2949 (2023)
52. Clemmer, D.E., Russell, D.H., Williams, E.R.: Characterizing the Conformationome: Toward a Structural Understanding of the Proteome. *Accounts Chem. Res.* **50**, 556-560 (2017)
53. Karch, K.R., Snyder, D.T., Harvey, S.R., Wysocki, V.H.: Native Mass Spectrometry: Recent Progress and Remaining Challenges. *Ann. Rev. Biophys.* **51**, 157-179 (2022)
54. Bakhtiari, M., Konermann, L.: Protein Ions Generated by Native Electrospray Ionization: Comparison of Gas Phase, Solution, and Crystal Structures. *J. Phys. Chem. B* **123**, 1784-1796 (2019)
55. Wyttenbach, T., Bowers, M.T.: Structural Stability from Solution to the Gas Phase: Native Solution Structure of Ubiquitin Survives Analysis in a Solvent-Free Ion Mobility–Mass Spectrometry Environment. *J. Phys. Chem. B* **115**, 12266-12275 (2011)
56. Breuker, K., Brüschweiler, S., Tollinger, M.: Electrostatic Stabilization of a Native Protein Structure in the Gas Phase. *Angew. Chem. Int. Ed.* **50**, 873-877 (2011)
57. Bleiholder, C., Liu, F.C.: Structure Relaxation Approximation (SRA) for Elucidation of Protein Structures from Ion Mobility Measurements. *J. Phys. Chem. B* **123**, 2756-2769 (2019)
58. Shelimov, K.B., Clemmer, D.E., Hudgins, R.R., Jarrold, M.F.: Protein Structure in Vacuo: The Gas-Phase Conformation of BPTI and Cytochrome c. *J. Am. Chem. Soc.* **119**, 2240-2248 (1997)
59. Dixit, S.M., Polasky, D.A., Ruotolo, B.T.: Collision induced unfolding of isolated proteins in the gas phase: past, present, and future. *Curr. Opin. Chem. Biol.* **42**, 93-100 (2018)
60. Nouchikian, L., Lento, C., Donovan, K.A., Dobson, R.C., Wilson, D.J.: Comparing the Conformational Stability of Pyruvate Kinase in the Gas Phase and in Solution. *J. Am. Soc. Mass Spectrom.* **31**, 685-692 (2020)
61. Hopper, J.T.S., Oldham, N.J.: Collision Induced Unfolding of Protein Ions in the Gas Phase Studied by Ion Mobility-Mass Spectrometry: The Effect of Ligand Binding on Conformational Stability. *J. Am. Soc. Mass Spectrom.* **20**, 1851-1858 (2009)
62. Donor, M.T., Shepherd, S.O., Prell, J.S.: Rapid Determination of Activation Energies for Gas-Phase Protein Unfolding and Dissociation in a Q-IM-ToF Mass Spectrometer. *J. Am. Soc. Mass Spectrom.* **31**, 602-610 (2020)
63. Zheng, X.Y., Kurulugama, R.T., Laganowsky, A., Russell, D.H.: Collision-Induced Unfolding Studies of Proteins and Protein Complexes using Drift Tube Ion Mobility-Mass Spectrometer. *Anal. Chem.* **92**, 7218-7225 (2020)
64. Borotto, N.B., Osho, K.E., Richards, T.K., Graham, K.A.: Collision-Induced Unfolding of Native-like Protein Ions Within a Trapped Ion Mobility Spectrometry Device. *J. Am. Soc. Mass Spectrom.* **33**, 83-89 (2022)

65. Gadkari, V.V., Ramirez, C.R., Vallejo, D.D., Kurulugama, R.T., Fjeldsted, J.C., Ruotolo, B.T.: Enhanced Collision Induced Unfolding and Electron Capture Dissociation of Native-like Protein Ions. *Anal. Chem.* **92**, 15489-15496 (2020)
66. Glasoe, P.K., Long, F.A.: Use of glass electrodes to measure acidities in deuterium oxide. *J. Phys. Chem.* **64**, 188-190 (1960)
67. Wintrode, P.L., Makhatadze, G.I., Privalov, P.L.: Thermodynamics of Ubiquitin Unfolding. *Proteins: Struct. Funct. Genet.* **18**, 246-253 (1994)
68. Greenfield, N.J.: Using circular dichroism spectra to estimate protein secondary structure. *Nat. Protoc.* **1**, 2876-2890 (2006)
69. Swint, L., Robertson, A.D.: Thermodynamics of unfolding for turkey ovomucoid third domain: Thermal and chemical denaturation. *Protein Sci.* **2**, 2037-2049 (1993)
70. Rodger, A. Far UV Protein Circular Dichroism. In *Encyclopedia of Biophysics*; Roberts, G. C. K. Ed.; Springer Berlin Heidelberg: Berlin, Heidelberg, 2013; pp. 726-730.
71. Privalov, P.L., Khechinashvili, N.N.: A Thermodynamic Approach to the Problem of Stabilization of Globular Protein Structure: A Calorimetric Study. *J. Mol. Biol.* **86**, 665-684 (1974)
72. Douglas, D.J.: Applications of collision dynamics in quadrupole mass spectrometry. *J. Am. Soc. Mass Spectrom.* **9**, 101-113 (1998)
73. Mayer, P.M., Poon, C.: The Mechanism of Collisional Activation of Ions in Mass Spectrometry. *Mass Spectrom. Rev.* **28**, 608-639 (2009)
74. Sun, Y., Vahidi, S., Sowole, M.A., Konermann, L.: Protein Structural Studies by Traveling Wave Ion Mobility Spectrometry: A Critical Look at Electrospray Sources and Calibration Issues. *J. Am. Soc. Mass Spectrom.* **27**, 31-40 (2016)
75. Gabelica, V., Shvartsburg, A.A., Afonso, C., Barran, P., Benesch, J.L.P., Bleiholder, C., Bowers, M.T., Bilbao, A., Bush, M.F., Campbell, J.L., Campuzano, I.D.G., Causon, T., Clowers, B.H., Creaser, C.S., De Pauw, E., Far, J., Fernandez-Lima, F., Fjeldsted, J.C., Giles, K., Groessl, M., Hogan, C.J., Hann, S., Kim, H.I., Kurulugama, R.T., May, J.C., McLean, J.A., Pagel, K., Richardson, K., Ridgeway, M.E., Rosu, F., Sobott, F., Thalassinos, K., Valentine, S.J., Wytenbach, T.: Recommendations for reporting ion mobility Mass Spectrometry measurements. *Mass Spectrom. Rev.* **38**, 291-320 (2019)
76. Grandori, R.: Detecting equilibrium cytochrome *c* folding intermediates by electrospray ionization mass spectrometry: Two partially folded forms populate the molten globule state. *Protein Sci.* **11**, 453-458 (2002)
77. Chowdhury, S.K., Katta, V., Chait, B.T.: Probing Conformational Changes in Proteins by Mass Spectrometry. *J. Am. Chem. Soc.* **112**, 9012-9013 (1990)
78. Shi, H., Atlasevich, N., Merenbloom, S.I., Clemmer, D.E.: Solution Dependence of the Collisional Activation of Ubiquitin [M + 7H]<sup>7+</sup> Ions. *J. Am. Soc. Mass Spectrom.* **25**, 2000-2008 (2014)
79. Bonner, J.G., Lyon, Y.A., Nellesen, C., Julian, R.R.: Photoelectron Transfer Dissociation Reveals Surprising Favorability of Zwitterionic States in Large Gaseous Peptides and Proteins. *J. Am. Chem. Soc.* **139**, 10286-10293 (2017)

80. Fink, A.L., Calciano, L.J., Goto, Y., Kurotso, T., Palleros, D.R.: Classification of Acid Denaturation of Proteins: Intermediates and unfolded states. *Biochemistry* **33**, 12504-12511 (1994)
81. Konermann, L., Metwally, H., Duez, Q., Peters, I.: Charging and Supercharging of Proteins for Mass Spectrometry: Recent Insights into the Mechanisms of Electrospray Ionization. *Analyst* **144**, 6157-6171 (2019)
82. Kaltashov, I.A., Abzalimov, R.R.: Do Ionic Charges in ESI MS Provide Useful Information on Macromolecular Structure? *J. Am. Soc. Mass Spectrom.* **19**, 1239-1246 (2008)
83. Katta, V., Chait, B.T.: Hydrogen/Deuterium Exchange Electrospray Ionisation Mass Spectrometry: A Method for Probing Protein Conformational Changes in Solution. *J. Am. Chem. Soc.* **115**, 6317-6321 (1993)
84. Guttman, M., Wales, T.E., Whittington, D., Engen, J.R., Brown, J.M., Lee, K.K.: Tuning a High Transmission Ion Guide to Prevent Gas-Phase Proton Exchange During H/D Exchange MS Analysis. *J. Am. Soc. Mass Spectrom.* **27**, 662-668 (2016)
85. Bundi, A., Wuthrich, K.: H-1-NMR parameters of the common amino acid residues measured in aqueous solutions of the linear tetrapeptides H-Gly-Gly-X-L-Ala-OH. *Biopolymers* **18**, 285-297 (1979)
86. Donor, M.T., Mroz, A., Prell, J.S.: Experimental and theoretical investigation of overall energy deposition in surface-induced unfolding of protein ions. *Chem. Sci.* **10**, 4097-4106 (2019)
87. Konermann, L., Aliyari, E., Lee, J.H.: Mobile Protons Limit the Stability of Salt Bridges in the Gas Phase: Implications for the Structures of Electrosprayed Protein Ions. *J. Phys. Chem B* **125**, 3803-3814 (2021)
88. Zhang, Z., Browne, S.J., Vachet, R.W.: Exploring Salt Bridge Structures of Gas-Phase Protein Ions using Multiple Stages of Electron Transfer and Collision Induced Dissociation. *J. Am. Soc. Mass Spectrom.* **25**, 604-613 (2014)
89. Zhou, M.W., Liu, W.J., Shaw, J.B.: Charge Movement and Structural Changes in the Gas-Phase Unfolding of Multimeric Protein Complexes Captured by Native Top-Down Mass Spectrometry. *Anal. Chem.* **92**, 1788-1795 (2020)
90. Bartman, C.E., Metwally, H., Konermann, L.: Effects of Multidentate Metal Interactions on the Structure of Collisionally Activated Proteins: Insights from Ion Mobility Spectrometry and Molecular Dynamics Simulations. *Anal. Chem.* **88**, 6905-6913 (2016)
91. Kazlauskas, R.: Engineering more stable proteins. *Chem. Soc. Rev.* **47**, 9026-9045 (2018)
92. Dill, K.A., Chan, H.S.: From Levinthal to pathways to funnels. *Nat. Struct. Biol.* **4**, 10-19 (1997)
93. Liu, L., Michelsen, K., Kitova, E.N., Schnier, P.D., Brown, A., Klassen, J.S.: Deuterium Kinetic Isotope Effects on the Dissociation of a Protein-Fatty Acid Complex in the Gas Phase. *J. Am. Chem. Soc.* **134**, 5931-5937 (2012)
94. Gao, S., Klinman, J.P.: Functional roles of enzyme dynamics in accelerating active site chemistry: Emerging techniques and changing concepts. *Curr. Op. Struct. Biol.* **75**, 102434 (2022)
95. Tajoddin, N.N., Konermann, L.: Structural Dynamics of a Thermally Stressed Monoclonal Antibody Characterized by Temperature-Dependent H/D Exchange Mass Spectrometry. *Anal. Chem.* **94**, 15499-15509 (2022)

96. Xiao, H., Hoerner, J.K., Eyles, S.J., Dobo, A., Voigtman, E., Mel'Cuk, A.I., Kaltashov, I.A.: Mapping protein energy landscapes with amide hydrogen exchange and mass spectrometry: I. A generalized model for a two-state protein and comparison with experiment. *Protein Sci.* **14**, 543-557 (2005)
97. Chaturvedi, R., Webb, I.K.: Multiplexed Conformationally Selective, Localized Gas-Phase Hydrogen Deuterium Exchange of Protein Ions Enabled by Transmission-Mode Electron Capture Dissociation. *Anal. Chem.* **94**, 8975–8982 (2022)
98. Pan, J., Heath, B.L., Jockusch, R.A., Konermann, L.: Structural Interrogation of Electrosprayed Peptide Ions by Gas-Phase H/D Exchange and Electron Capture Dissociation Mass Spectrometry. *Anal. Chem.* **84**, 373-378 (2012)
99. Karanji, A.K., Khakinejad, M., Kondalaji, S.G., Majuta, S.N., Attanayake, K., Valentine, J.S.: Comparison of Peptide Ion Conformers Arising from Non-Helical and Helical Peptides Using Ion Mobility Spectrometry and Gas-Phase Hydrogen/Deuterium Exchange. *J. Am. Soc. Mass Spectrom.* **29**, 2402-2412 (2018)
100. Rand, K.D., Pringle, S.D., Murphy, J.P., Fadgen, K.E., Brown, J., Engen, J.R.: Gas-Phase Hydrogen/Deuterium Exchange in a Traveling Wave Ion Guide for the Examination of Protein Conformations. *Anal. Chem.* **81**, 10019-10028 (2009)



## Table of Contents Figure

